Current source enhancements in Electrical Impedance Spectroscopy (EIS) to cancel unwanted capacitive effects

Ali Zarafshani*[a,c], Thomas Bach[b], Chris Chatwin[a] , Liangzhong Xiang[c] , and Bin Zheng[c]

[a] Bioelectrical Research Group, School of Eng. and Design, University of Sussex, UK, BN19QT; [b] Sensatech Research, Brighton, UK, BN2 0GP; [c] School of Electrical and Computer Eng., University of Oklahoma, Norman, OK, USA, 15213

ABSTRACT

Electrical Impedance Spectroscopy (EIS) has emerged as a non-invasive imaging modality to detect and quantify functional or electrical properties related to the suspicious tumors in cancer screening, diagnosis and prognosis assessment. A constraint on EIS systems is that the current excitation system suffers from the effects of stray capacitance having a major impact on the hardware subsystem as the EIS is an ill-posed inverse problem which depends on the noise level in EIS measured data and regularization parameter in the reconstruction algorithm. There is high complexity in the design of stable current sources, with stray capacitance reducing the output impedance and bandwidth of the system. To confront this, we have designed an EIS current source which eliminates the effect of stray capacitance and other impacts of the capacitance via a variable inductance. In this paper, we present a combination of operational CCII based on a generalized impedance converter (OCCII-GIC) with a current source. The aim of this study is to use the EIS system as a biomedical imaging technique, which is effective in the early detection of breast cancer. This article begins with the theoretical description of the EIS structure, current source topologies and proposes a current conveyor in application of a Gyrator to eliminate the current source limitations and its development followed by simulation and experimental results. We demonstrated that the new design could achieve a high output impedance over a 3MHz frequency bandwidth when compared to other types of GIC circuits combined with an improved Howland topology.

Keywords Biomedical Imaging equipment and instrument; electrical impedance spectroscopy (EIS); generalized impedance converter (GIC); current source.

1. INTRODUCTION

An Electrical Impedance Spectroscopy (EIS) image maps and describes electrical characteristic of biological tissues as a different form of data compared to other conventional medical imaging techniques. It allows to detect malignant tumors (e.g., breast cancer) at the early stage, thus it is called Electrical Impedance Mammography (EIM). The most recent techniques for the clinical and physiological applications of EIS systems is based on applying a known value of low amplitude current between 0.5mA to 2mA (less than 10mA in compliance with IEC60601-1, the general standard for medical equipment and medical systems). The current is injected to subject and measuring potentials at multi-frequency around 10 kHz to few megahertz, in order to produce impedance images of internal structures of the body for each frequency points. In regard to the advantages of the current source topologies i.e. predictability of constant current with the noise advantages, the current source are commonly employed on EIS systems as is utilized by Kyung Hee (IIRC & Mk1); Oxford Brookes (OXBACT5); Rensselaer (ACT4); Sheffield (Mk3.5); UCL (Mk2.5&1b) and also the Leicester group (Mk3) [1-7]. The enhancement of the EIS system focuses on developing electrical and electronic instrumentations to improve the accuracy of the transfer impedance measurements to make them operate up to high frequency for the purpose of measuring impedivity and conductivity of different tissues types [8-10]. The transfer impedance measurement is the ratio between current injections and voltage measurements obtained from the subject under test or a biological tissue sample to images the distribution of impedivity. Instability of the transfer impedance measurements is caused by circuit problems and field problems [11]. Figure 1 shows a simplified schematic of EIS system consists of digital-to-analogue convertor (DAC); voltage-to-current convertor (V/I); drive and receive multiplexers (DRV. Mux and REC. Mux); differential voltage amplifier (Diff. Amp.); programmable gain amplifier (PGA) and analogue-to-digital convertor (ADC) modules.

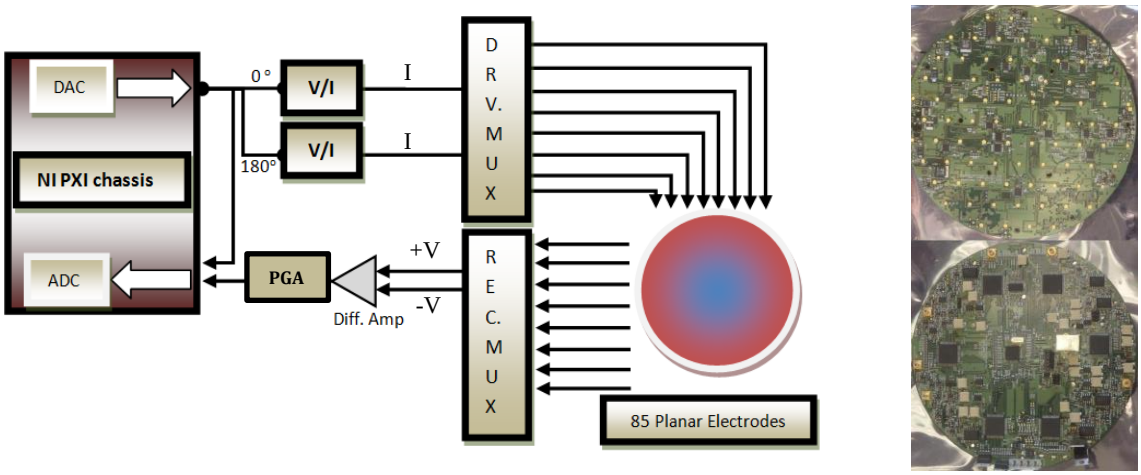

(a) (b)

Figure 1 (a) Overview of hardware block diagram of EIS system, (b) the bottom and the top sides of custom EIS board consisting of a planar 85-electrode plate at the bottom of the saline tank.

In our system, a single compact EIS circuit board consists of all EIS modules denoted by the hardware block diagram with a planar 85-electrode plate is designed as shown in Figure 1(b) [12-17]. This custom EIS board is placed at the bottom of the saline tank and the breast is immersed in a saline solution. The electrode plate is moved up to down to accommodate different sizes of breast where we can find the perfect position to maximize the number of electrodes covering the breast. The spring-loaded electrode is placed between the electrode pad and the breast is pressured to be able to cover as much as electrode possible and to overcome the contact impedance problem, as shown in Figure 2. In this structure, the electrode pads directly contact to current source circuit through multiplexers in order to remove any additional wire producing an extra stray capacitance.

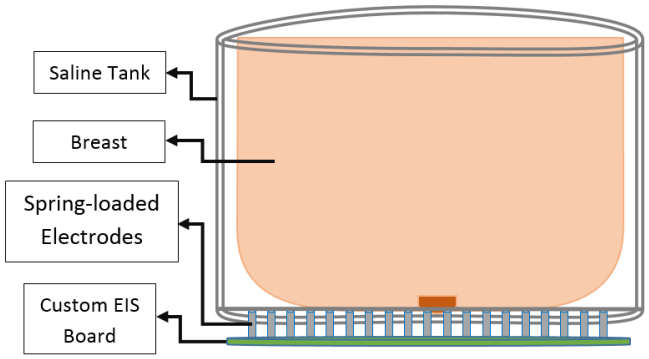

Figure 2 shows an EIS measurement tank with a planar electrode plate, in which the EIS board is placed at the bottom of the EIS measurement tank of 180×50mm diameter inside the clinical bed. The electrode will be placed between the electrode pad and the breast will be pressured to be able to cover as much as electrode possible.

The enhancement of the hardware subsystem of the EIS system focuses on developing electrical and electronic instrumentations and improving the source topologies to make them operate at multiple frequencies for the purpose of measuring permittivity and conductivity of different breast tissues. An ideal current excitation system is shown in the Figure 3, the output impedance (Z_O) shunts the source, thus should have infinite output impedance when the output resistance is ideally infinite and the output capacitance is negligible, thus $Z_O = R_O||C_O$.

In EIS system, high output impedance is required to avoid drawing away the current and to be able to pass the maximum known amount of the applied current through the subject. Therefore, the current excitation systems with

a low impedance output is a part of the circuit problems as a category of hardware systematic errors, thus for a given stable current source, it is important to reduce systematic errors with effective hardware design.

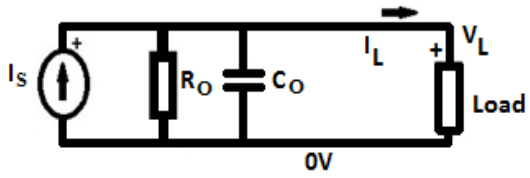

Figure 3. Ideal current source circuit with output resistance and capacitance parallel with the load resistance

Indeed, in order to achieve a high precision system, it is important that the current injection circuits have a high output impedance over the required frequency bandwidth. This will deliver a high-performance system with improved spatial resolution at high frequency, while the electrical properties of biological tissues change over a frequency range. However, in reality, the output impedance will not be infinite and the current source has affected by an unnecessary and useless extra capacitances that have generated between the electrical components on the printed circuit board (PCB). This is called stray or parasitic capacitance (C_{STRAY}) where it is in parallel with output capacitance of the source (Co) and load capacitance (C_L) and causes to reduce the total output impedance of the current source circuit, thus $Z_O=R_O||C_O+C_{STRAY}$. The stray capacitance is the key issue in the amount of output impedance of the current excitation system that reduces the frequency bandwidth of the entire system.

In addition, most of the EIS systems use cables to inject current whilst our compact EIS board is a single board including all modules with a planer electrode plate that able to apply the current signals with minimum noise. Our EIS system are mostly affected by on/off capacitance of the drive multiplexer switches plus parasitic capacitanace of the electrical components as denoted by C_X. This research has identified schemes to compensate for unwanted capacitances to facilitate high accurate and wideband EIS system.

2. MATERIALS AND METHODS

2.1 Improved Howland current source

Prof Bradford Howland in MIT made-up the basic Howland current source around 1962 that was published in 1964 by D.H. Sheingold [18]. The Howland current source is an excellent circuit to use for having a current source that can put out a current in either DC or AC with high output impedance and wide bandwidth range [19]. Regarding the output capability that does not normally swing very close to the rail, the “Improved” Howland source was recommended[19]. The improved Howland current source functions as a voltage controlled current source (VCCS) circuit. An Improved Howland current source topology using an op amp and consisting of 5 resistors which R_4 in Howland source is divided into R_{4a} and R_{4b} and the output node of the current source is between these two resistors, as shown in Figure 4. One of the most significant advantages of improved Howland current source compared to other sources is its ability to work at higher frequencies with removing (reduction of) the common-mode voltage or loading effects; so it can be concluded to use a current source that is based on the improved Howland circuit.

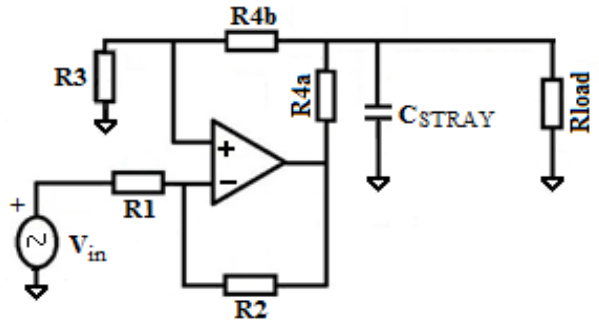

Figure. 4 The improved Howland current source

The output impedance of the improved Howland current source circuit is calculated by the following equation:

$$Z_O \equiv C_O \,||\, R_O = \frac{\frac{R_1}{R_2}.\frac{R_{4b}(R_3+R_{4a})}{(R_{4a}+R_{4b})}}{\frac{R_3}{(R_{4a}+R_{4b})}-\frac{R_1}{R_2}} \qquad 1$$

The maximum output impedance would not be achieved if there is a tolerance between any resistor R_1, R_2, R_{4a} and R_{4b} and two times of R_3. Therefore, it needs to match the ratio of R_1/R_2 and $R_3/(R_{4a}+R_{4b})$ to the maximum output impedance. According to the calculation, in equation (1), we can understand that the tolerance in resistors can cause altered in the output impedance of the current source. However, in practice, non-idealities from the op-amp limitations, resistor tolerances and the presence of stray capacitance in the design have the result of reducing output resistance and increasing output capacitance accordingly reducing output impedance of the current excitation system [20, 21]. The associated effective output capacitance of the current source and the parasitic capacitance create a total grounded capacitance that makes it impractical to produce an EIS system operating at high frequency. Thus, for utilizing the improved Howland current source of high frequency recommend using a stray capacitance cancellation method of producing the inductance in parallel with the total stray capacitance. Thus, an inductance in parallel with the stray capacitance and source realized by an RLC circuit. This provided a way to reduce the stray capacitance effect at high frequency.

2.2 Stray capacitance cancellation method based on CCII

There are active network synthesizers in the practical design employing various active devices such as current conveyor (CC) and passive elements in their functions. We suggested operational second generation current conveyor in the GIC form. The GIC based on OCCII, here is called OCCII-GIC structure. The CCIIs are used for the GIC due to their attractive inductive behavior, which is dependent on the impedance structure of the output current of the CCII for capacitance compensation. This GIC form is used to provide an inductance without any matching constraint, using minimum grounded passive components.

In order to have a multi-frequency system, the OCCII as an active component in the gyrator form employs digital-pots to provide a variable inductance without any matching constraint. We present this new OCCII-GIC technique for cancellation of the parasitic elements in multi-frequency current excitation for the EIS systems. Figure 5 shows the schematic of a grounded inductor based on the OCCII whereas the conductance Y_3 and Y_4 are variable resistors and Y_1 is a capacitor. Therefore, the input impedance ideally acts as a pure inductor $Z_{in} = sL = sC_1 \times R_3 \times R_4$.

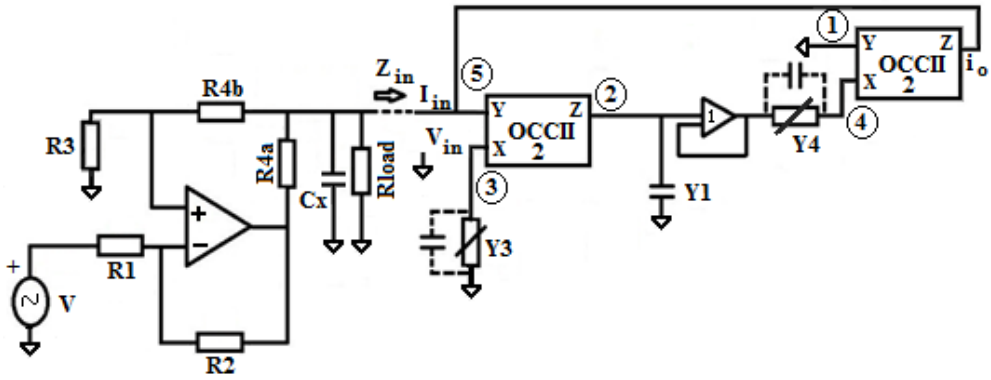

Figure 5. An improved schematic of an OCCII-GIC as a grounded inductor combined with the improved Howland current source to cancel the total grounded parasitic capacitance (denoted by C_X) effects. We replaced digit-pots for admittance of Y_3 and Y_4 as well as a capacitance for admittance of Y_1 in the OCCII-GIC topology in order to produce a variable grounded inductance.

There are limitations to produce a pure inductance in the multi-frequency system because of using digital-pots. Each digital-pot (replacement of resistor) naturally come with grounded capacitance at both ends and parallel capacitance at the wiper. Thus, the following equations are computed to consider the act of OCCII-GIC circuit caused by the digital-pots, as the digital-pot swings from 1 to the full-scale value to operate in multi-frequency systems, thus, $Y_1 = sC_1$, $Y_3 = G_3 + sC_{ground-3}$ and $Y_4 = G_4 + sC_{wiper-4}$, we can write:

$$Z_{in} = \frac{V_{in}}{I_{in}} = \frac{Y_1}{Y_3 Y_4} = \frac{sC_1}{(G_3 + sC_{ground-3})(G_4 + sC_{wiper-4})} = \frac{sC_1}{(G_3.G_4 - C_{ground-3}.C_{wiper-4})} + \frac{C_1}{(G_4.C_{ground-3} + G_3.C_{wiper-4})} \quad (2)$$

whereas equivalent inductance and ground resistance parallel with output resistance can calculated as follows:

$$L_{eq} = \frac{sC_1}{(G_3.G_4 - C_{ground-3}.C_{wiper-4})} \quad (3)$$

$$R_{eq} = \frac{C_1}{(G_4.C_{ground-3} + G_3.C_{wiper-4})} \quad (4)$$

Thus, the RLC parallel circuit is implemented when an OCCII-GIC parallels with the output of a current source circuit.

3. RESULTS

In the 1st step, we simulated a mirrored structure of improved Howland current source combined with two OCCII-GIC circuits in order to cancel dummy stray capacitance in each branch. Each current branch is switched between 85 electrodes. The drive multiplexer uses a cascading method to reduce the on/off capacitance of the drive

multiplexer.to 20.8pF involved in each injection channel. Therefore, two OCCII-GICs are used for the two 180 degrees out of phase current branches (mirror current source structure) for stray capacitance cancellation. The combination of schematic of current sources with OCCII-GIC topology is simulated in OrCAD Capture release 16.6 PSpice A/D 16.2.0, with a spice Micro-Model of the AD844 *Rev. A* and OPA656 *Rev. A*. The actual resistance tolerance of 0.01% used in our EIT system then is paralleled with a capacitance of 0.3pF that in reality is created by a circuit board.

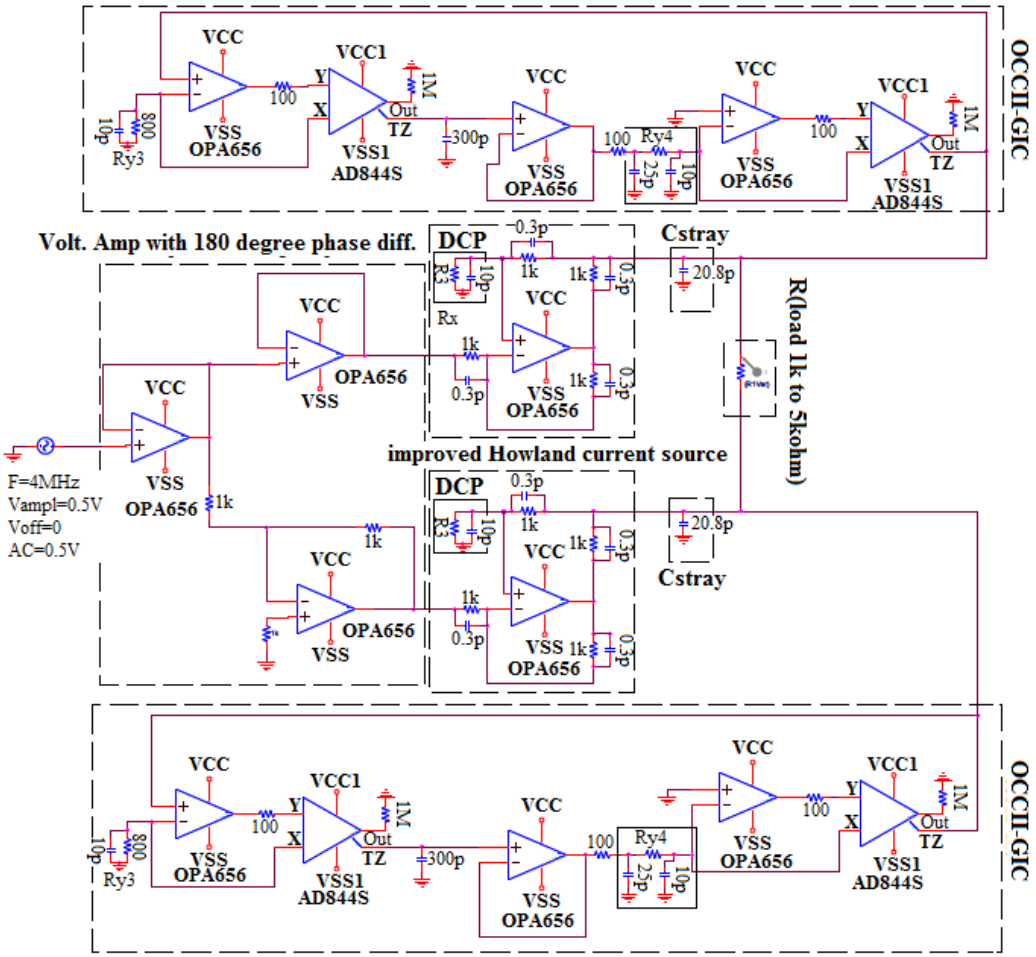

Figure 6. (a) Simulation schematic of the mirrored improved Howland current source by utilizing two OCCII-GIC circuits with actual component values to cancel dummy stray and parasitic capacitance values.

The current source simulations were run for different loads with a variable load of R_{VAR} (load) from 1kΩ up to 5kΩ. The AC sweep and time domain analysis results show the possibility of the stray capacitance cancelation method combined with the current source for the high-frequency EIS systems, as shown in Figure.

We consider the effect of digital-pots on the use of capacitance cancellation method for the floating and grounded admittances, Y_3 and Y_4. In the case of the grounded admittance Y_3, the equivalent admittance is consisted of a resistance parallel with a digital-pot low pins grounded capacitance, $Z_3=R_{Y3}||C_{Y3}$. In the case of floating admittance Y_4, the equivalent admittance is consisted of a float resistor with the high and wiper pin capacitance of digital-pot, $Z_4=R_{Y4}||C_W$ and C_H, when the low pin is floated.

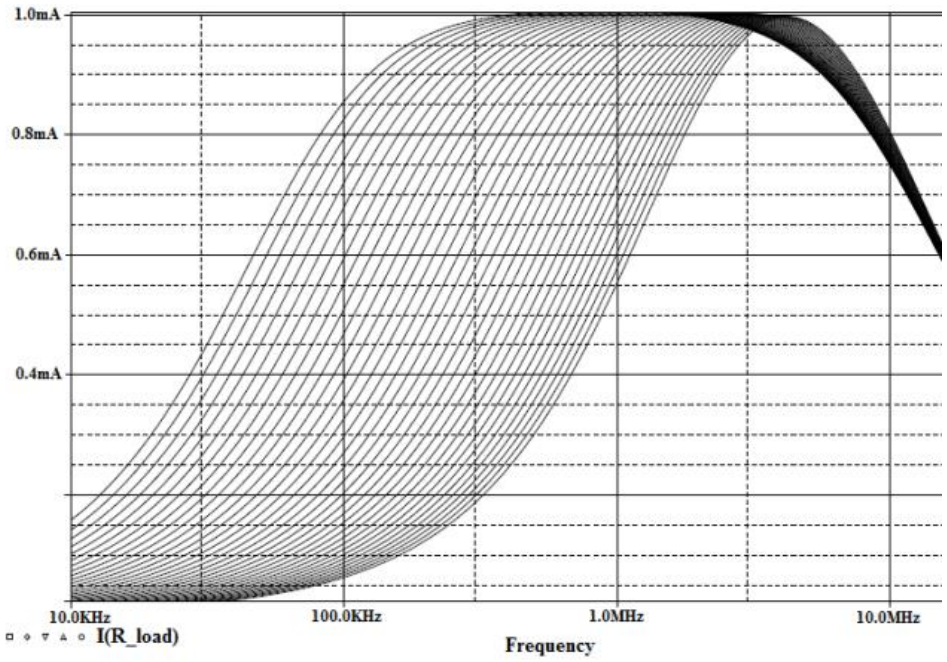
1.0mA
0.8mA
0.6mA
0.4mA
10.0KHz
100.0KHz
1.0MHz
10.0MHz
I(R_load)
Frequency

(a)

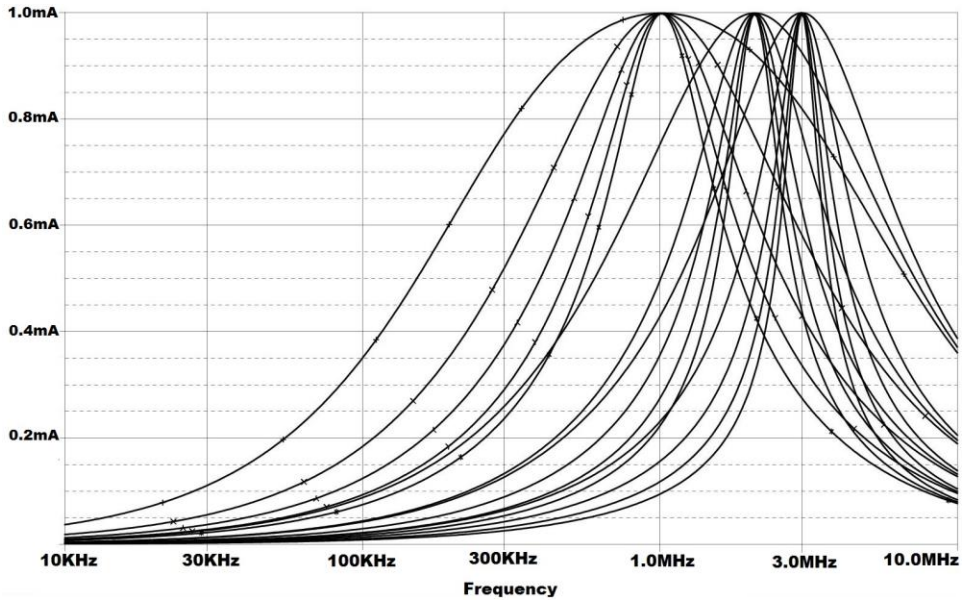
1.0mA
0.8mA
0.6mA
0.4mA
0.2mA
10KHz
30KHz
100KHz
300KHz
1.0MHz
3.0MHz
10.0MHz
Frequency

(b)

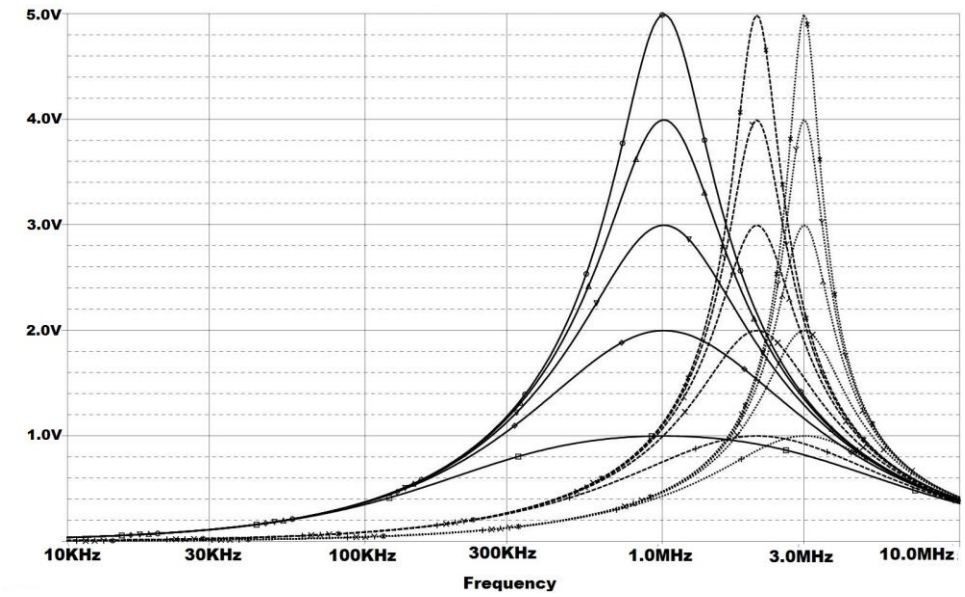

(c)

Figure 7 (a) the simulation graph shows a multi-frequency AC sweep output current. Digital-pot Y_4 sets from 100Ω to 5kΩ, increment in 10 logarithmic steps per decade, (b) the simulation graph shows the AC sweep output current at three different sample frequency points from 1MHz, 2MHz, 3MHz for different loads from 1kΩ to 5kΩ, wide to narrow curve and (c) the graph shows the output voltage from $1V^{AC}$ to $5V^{AC}$ corresponding to different loads (a variable load from R_{VAR}= 1kΩ up to 5kΩ).

In the 2nd step, we assessed the EIS system by measuring the output impedance of the current source under test. A plot of the output impedance versus different frequency points is provided as shown in Figure 8. We assign the resulting maximum value of R_O when minimizing the output capacitance C_O of the circuit, thus resulting maximum value of output impedance of the excitation system Z_O. We maximized the output impedance of the current source by using the digital-pot inside the improved Howland current source, in place of R_3, and eliminated the total output capacitance by adjusting the digital-pot inside the OCCII-GIC, in place of Y_4 admittance. Although the output impedance is influenced by the both digital-pots in the improved Howland source and the OCCII-GIC because of digital-pot pin capacitance, so the maximum output impedance of the current excitation is achieved when these influences are cancel each other in the mirror source structure for a specific frequency point. The digital-pots in OCCII-GIC are adjusted to eliminate the total output capacitance C_O=3fF (femto-Farad), thus, an output impedance of 5MΩ at the 3MHz frequency point has been achieved. Although a phase shift is present in the current output signals and it needs to be computed as a part of the measurement data when producing the image.

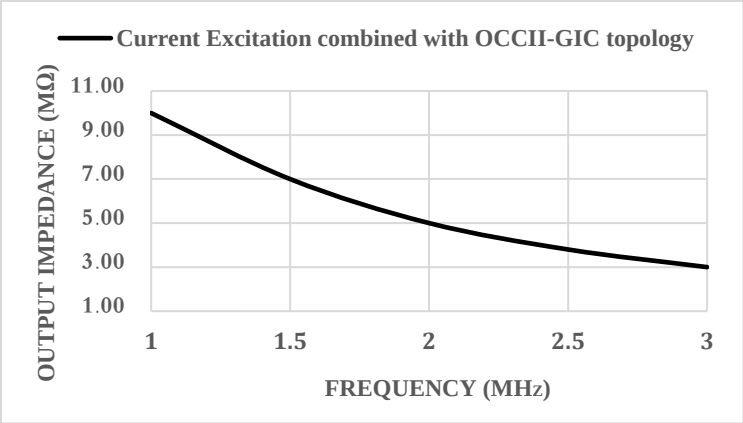

Figure 8 shows the output impedance (Z_O) when combining the current excitation system with OCCII-GIC topology as a capacitance cancellation method over the desired frequency bandwidth up to 3MHz.

4. DISCUSSION

In response to the need to increase the chances of detecting cancer at an early stage, which is directly related to improve survival of patients with respect to the increasing number of cancer cases, in this study we presented an EIM system and investigated a number of issues to develop high accurate and wide bandwidth excitation system resulting to improve image quality of this new imaging modality. By emphasizing non-invasive imaging techniques for clinical application in screening program, we have designed and developed a new EIM system that operates at high frequencies with low noise and high precision analogue circuits sufficient to inject current with unwanted low capacitive effects and measure the voltage needed to reconstruct impedance images.

The key characteristics of the current source for EIT systems are the ability to produce a stable constant current and obtain high output impedance during a range of low and high frequencies. We used improved Howland current source as main current injection topologies in bio-impedance measurement systems. Thus, the important parameter of a current source in EIS system is its output impedance depends on its gain, frequency bandwidth, output resistance, and output capacitance. However, the current excitation system effects with all parasitic capacitance at the electrode level, and crosstalk at the chip and PCB level as well as on/off capacitance of the drive multiplexers. In this study, a multi-frequency current excitation system with the stray capacitance cancellation method for EIS systems is developed by utilizing OCCII-GIC topology and digital-pots to operate as variable admittances for producing the variable inductor corresponding to different frequency point. This configuration has many advantages over other excitation systems especially allows to minimum and calculate the stray capacitance effects of the single source structure and high stability with low noise for EIT systems.

A new feature of the gyrator circuit based on current conveyors has been presented with voltage-based source topology. This capacitance cancellation technique is capable of working with other existing (current-based and voltage-based) EIS excitation systems such as operational trans-conductance amplifier source, general impedance converter source, Wien Bridge circuit, Wien Bridge circuit with voltage to current converter circuit and current conveyor current sources. The study results of the OCCII-GIC are based on the active device with a current feedback loop, thus it is feasible to tune over a wide range of parameters. This is a significant change in the EIS design compared to the general current source methods used to ameliorate the constraints caused by passive components and op amp limitations.

To the best of the authors' knowledge, there has not been any practical system using inductance to cancel the effect of capacitances of the current source above the 500 kHz range with acceptable output impedance for the EIS systems. Comparison of the criteria used by Ross (ACT4) [2] and Oh (KHU) [7, 22] EIT systems show a similar method

to cancel the stray capacitance by producing inductance. However, different circuits based on general GIC structure consists of two op amps and five passive components are used. Their works also utilized digital-pots to produce a multi frequency system establishing an EIS system that works at frequency up to 500 kHz. However, using a digital-pot is naturally produced parallel grounded capacitors in high and low pins and a wiper with a variable resistor as directly reduces entire current source output impedance which was not consider in their design. Also the research by Oh [22]has embedded six general GIC structures, identical in structure but with different values. These general GIc structures assigned to different frequency ranges in order to achieve the same effect at six different frequencies by switching between the different GICs and balancing the equivalent output resistor. However, the implemented results show it is extremely difficult to achieve an output impedance exceeding 1MΩ for the frequency upper than 500 kHz. The advantages of using six GICs, as reported by Oh[7, 22], must be set against the high component count, instability with composite waveforms as well as the complex circuitry caused by op amps, using five passive components and other capacitance effects. The passive components for the general GIC structure are available with a tolerance and each of the five passive component in reality is paralleled with an estimated capacitance on the circuit board. Moreover, op amps are affected by the common-mode and differential input impedance which is undetermined in their study.

For a given stable and known current injection with stray capacitance of the system, it is important to reduce systematic errors with an effective hardware design. Thus, our focus was first on reducing the effect of on/off capacitance of the drive multiplexers using a cascading method. Also in our planar EIS system, electrodes directly connected to current injection without any extra wiring to minimize and to fix the stray capacitance of the system. This increase the ability to produce good spatial resolution when the system involved with the predictable values. Finally, we proposed to use a capacitance cancellation circuit to reduce the effective capacitance to comply with the required output impedance. Therefore, producing a fixed and stable values and improvement of system sensitivity, reliability and reproducibility.

In summary, this study concentrates on the design, development and calibration of a high performance EIM system for early detection of breast cancer applicable for different breast sizes and shapes. A constraint on EIS systems is that the current injection suffers from the effects of stray capacitance having a major impact on the hardware as the EIS is an ill-posed inverse problem which depends on the noise level in the measured data and regularization parameter in the reconstruction algorithm. The research aim was to prevent this problem by using a capacitance cancellation method and calibration methods to facilitate operation in the high frequency range.

5. ACKNOWLEDGEMENT

This work is supported in part by Innovative grant, University of Sussex, England. The authors would also like to acknowledge the support from the Peggy and Charles Stephenson Cancer Center, University of Oklahoma, OK, US.

VI. REFERENCES

[1] Hartov, A., Mazzarese, R. A., Reiss, F. R., Kerner, T. E., Osterman, K. S., Williams, D. B. and Paulsen, K. D. , "A multichannel continuously selectable multifrequency electrical impedance spectroscopy measurement system," IEEE Transactions on Biomedical Engineering 47(1), 49-58 (2000).

[2] Ross, A. S., Saulnier, G., Newell, J. and Isaacson, D., "Current source design for electrical impedance tomography," Physiol.Meas. 24(2), 509 (2003).

[3] Wilson, A., Milnes, P., Waterworth, A., Smallwood, R. and Brown, B. , "Mk3. 5: a modular, multi-frequency successor to the Mk3a EIS/EIT system," Physiol.Meas. 22(1), 49 (2001).

[4] McEwan, A., Romsauerova, A., Yerworth, R., Horesh, L., Bayford, R. and Holder, D. , "Design and calibration of a compact multi-frequency EIT system for acute stroke imaging," Physiol.Meas. 27(5), S199 (2006).

[5] Bayford, R. , "Bioimpedance tomography (electrical impedance tomography)," Annu.Rev.Biomed.Eng. 8, 63-91 (2006).

[6] Fabrizi, L., McEwan, A., Oh, T., Woo, E. and Holder, D. , "A comparison of two EIT systems suitable for imaging impedance changes in epilepsy," Physiol.Meas. 30(6), S103 (2009).

[7] Oh, T. I., Lee, K. H., Kim, S. M., Koo, H., Woo, E. J. and Holder, D. , "Calibration methods for a multi-channel multi-frequency EIT system," Physiol.Meas. 28(10), 1175 (2007).

[8] McEwan, A., Cusick, G. and Holder, D. , "A review of errors in multi-frequency EIT instrumentation," Physiol.Meas. 28(7), S197 (2007).

[9] Mahnam, A., Yazdanian, H. and Samani, M. M. , "Comprehensive study of Howland circuit with non-ideal components to design high performance current pumps," Measurement 82, 94-104 (2016).

[10] Bouchaala, D., Kanoun, O. and Derbel, N. , "High accurate and wideband current excitation for bioimpedance health monitoring systems," Measurement 79, 339-348 (2016).

[11] Brown, B. H. , "Electrical impedance tomography (EIT): a review," J.Med.Eng.Technol. 27(3), 97-108 (2003).

[12] Zarafshani, A. A high-performance, multi-frequency micro-controlled Electrical Impedance Mammography (EIM) excitation and phantom validation system (2016).

[13] Zarafshani, A., Huber, N., Béqo, N., Tunstall, B., Sze, G., Chatwin, C. and Wang, W., "A flexible low-cost, high-precision, single interface electrical impedance tomography system for breast cancer detection using FPGA," Journal of Physics: Conference Series, 012169 (2010).

[14] Zarafshani, A., Qureshi, T., Bach, T., Chatwin, C. and Soleimani, M., "A 3D Multi-frequency response electrical mesh phantom for validation of the planar structure EIT system performance," Electro Information Technology (EIT), 2016 IEEE International Conference on, 0600-0604 (2016).

[15] Zarafshani, A. , "A high-performance, multi-frequency micro-controlled Electrical Impedance Mammography (EIM) excitation and phantom validation system," Doctoral dissertation, University of Sussex, Brighton, East Sussex, UK (2016).

[16] Qureshi, T., Chatwin, C., Huber, N., Zarafshani, A., Tunstall, B. and Wang, W., "Comparison of Howland and General Impedance Converter (GIC) circuit based current sources for bio-impedance measurements," Journal of Physics: Conference Series, 012167 (2010).

[17] Zhang, X., Wang, W., Sze, G., Barber, D. and Chatwin, C. , "An image reconstruction algorithm for 3-D electrical impedance mammography," IEEE Trans.Med.Imaging 33(12), 2223-2241 (2014).

[18] Sheingold, D. , "Impedance & admittance transformations using operational amplifiers," The Lightning Empiricist 12(1), 4 (1964).

[19] Pease, R. A. , "A comprehensive study of the Howland current pump," National Semiconductor (2008).

[20] Cook, R. D., Saulnier, G. J., Gisser, D. G., Goble, J. C., Newell, J. and Isaacson, D. , "ACT3: a high-speed, high-precision electrical impedance tomograph," IEEE Transactions on Biomedical Engineering 41(8), 713-722 (1994).

[21] Pease, R. A. , "A comprehensive study of the Howland current pump," National Semiconductor (2008).

[22] Oh, T. I., Wi, H., Kim, D. Y., Yoo, P. J. and Woo, E. J. , "A fully parallel multi-frequency EIT system with flexible electrode configuration: KHU Mark2," Physiol.Meas. 32(7), 835 (2011).